Estimating Cloud Type from Pyranometer Observations

CLAUDE E. DUCHON AND MARK S. O'MALLEY

School of Meteorology, University of Oklahoma, Norman, Oklahoma

(Manuscript received 29 September 1997, in final form 15 March 1998)

ABSTRACT

In this paper the authors evaluate an inexpensive and automatable method to estimate cloud type at a given location during daylight hours using the time series of irradiance from a pyranometer. The motivation for this investigation is to provide ground-based estimates of cloud type at locations where there are no human observations of sky condition. A pyranometer naturally measures the effect of intervening clouds along the solar beam path to the sensor. Because a daily time series of irradiance is nonstationary, it is appropriately scaled to yield a stationary time series. From the latter, the standard deviation and ratio of observed irradiance to clear-sky irradiance derived from a 21-min moving window are related to one of the following cloud types or conditions: cirrus, cumulus, cirrus and cumulus, stratus, precipitation or fog, no clouds, and other clouds. Comparisons with human observations at the Department of Energy Atmospheric Radiation Measurement Calibration and Radiation Testbed site in northern Oklahoma show that the pyranometer method and human observations are in agreement about 45% of the time. Many of the differences can be attributed to two factors: 1) the pyranometer method is weighted toward clouds crossing the sun's path, while the human observer can view clouds over the entire sky, and 2) the presence of aerosols causes the pyranometer to overestimate the occurrence of cirrus and cirrus plus cumulus. When attenuation of the solar beam by aerosols is negligible or can be accounted for, the pyranometer method should be especially useful for cloud-type assessment where no other sky observations are available.

1. Introduction

Knowledge of sky condition is a natural element that describes the current weather at a given location. Other standard elements are temperature, wind speed, wind direction, etc. Ground-based cloud information is best obtained from a human observer at the location. This is in contrast to most other elements that can be accurately measured with instrumentation. When there is no observer present, other means of determining cloud conditions can be considered. One is the use of satellite imagery. With computer access to geostationary and polar orbiter satellite data one can employ both visible and infrared wavelengths to assess cloudiness on various spatial and temporal scales.

However, access to satellite data is not universal. In circumstances where current cloud information is desired for remote locations there is an alternative method to consider—a ground-based one. Thus the purpose of this paper is to explore the potential for using a pyranometer to determine a number of the major cloud types occurring at the measurement site during daylight hours using simple statistics (mean and variance) derived from the time series of pyranometer irradiance. Possible uses of cloud-type data include general aviation operational needs, a supplement to the Automated Surface Observing System (ASOS), determining clouds over snow-covered surfaces, and with widespread use, for comparison to the International Satellite Cloud Climatology Project (ISCCP) cloud-type estimates. With regard to the first application, knowledge of the presence of stratus, fog or precipitation, cumulus, or clear skies could be useful to pilots flying to landing strips or airports where no other present weather observations are taken. Since ASOS sky condition measurements (ceiling and cloud amount) are limited to a maximum height of 12 000 ft, the addition of a pyranometer could provide cloud type both above and below this height. As pointed out by Bland (1996), satellite estimates of surface insolation (and thus cloudiness) over snow-covered surfaces are problematic. A properly heated and ventilated pyranometer should yield useful cloud information in this situation.

With regard to ISCCP, the cloud types determined in this paper could be compared with the cloud types estimated from satellite radiances (Fig. 4 in Rossow and Schiffer 1991). However, for comparison purposes the ISCCP 30-km mapped pixels must be used, not the 280-km resolution. As shown recently by Barnett et al. (1998) for clear and cloudy skies, the correlation between surface-measured solar irradiance at a point and

Corresponding author address: Prof. Claude E. Duchon, School of Meteorology, University of Oklahoma, 1310 Energy Center, 100 East Boyd, Norman, OK 73019-0470.
E-mail: cduchon@ou.edu

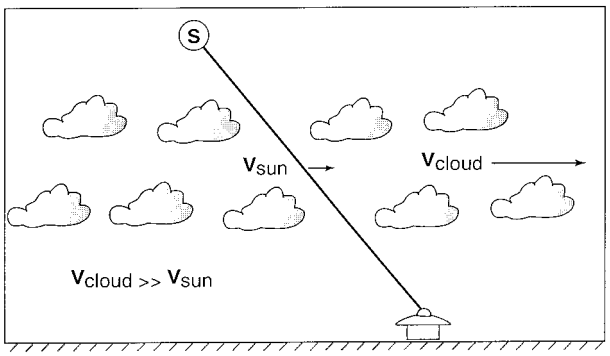

FIG. 1. The basis for using a pyranometer to estimate cloud type is that the clouds cross the solar beam impinging on the sensor, thus providing a time series of global irradiance fluctuations due to clouds.

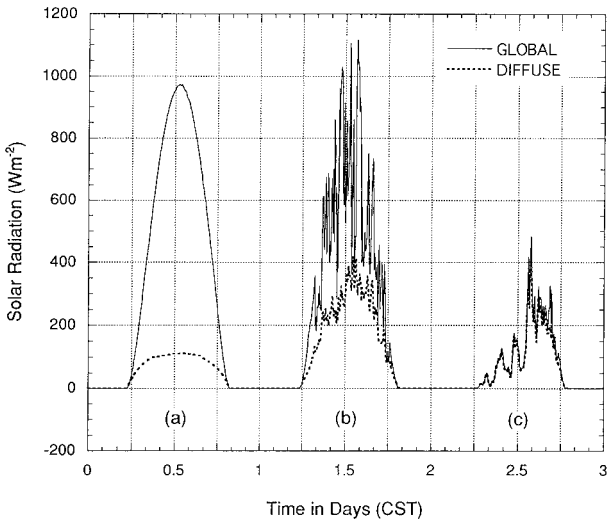

FIG. 2. Comparison of diffuse and global irradiance for (a) a clear day, (b) a partly cloudy day, and (c) a mostly cloudy day at Norman, OK, for 12 July, 5 August, and 11 September 1995, respectively.

the average irradiance of surrounding stations is about 0.9 (80% variance in common) for an area within a 30-km radius and decreases rapidly as the radius increases. The average station spacing in the Oklahoma Mesonet (Brock et al. 1995) is between 30 and 35 km (the data source from which Barnett et al. 1998 performed their analysis) so that an interesting study comparing ISCCP and pyranometer cloud-type estimates might be performed.

It seems obvious at the outset that the inclusion of other atmospheric radiation measurements such as diffuse, direct, and atmospheric soundings can only improve the estimation of cloud type derived from a single instrument. However, the additional instrumentation is available only at a few locations, for example, the Department of Energy Atmospheric Radiation Measurement (ARM) sites in Oklahoma, Alaska, and the southwest Pacific. Our interest here is predicated on taking advantage of the good accuracy, simplicity, low cost, robustness, and minimum maintenance associated with state-of-the-art pyranometers.

The outline of the remainder of the paper is as follows: section 2 provides the basis for using a pyranometer to estimate cloud type, section 3 discusses the irradiance-based classification method, section 4 describes the clear-sky irradiance model for standardizing irradiance measurements, and sections 5 and 6 compare irradiance-based cloud-type estimates with human observations of cloud type. A summary and conclusions are given in section 7.

2. Pyranometer response to clouds

A pyranometer measures the hemispheric broadband solar radiation available to drive the daytime surface energy budget. These measurements naturally integrate the effects of clouds. The concept of using a pyranometer to estimate cloud type is illustrated in Fig. 1 in which comparatively fast-moving clouds cross the slow-moving path of the solar beam. For cloud bases at 1 km the speed of the solar beam varies from 0.07 overhead to 2.4 m s^{-1} at a zenith angle of 80°, while at a cloud base of 10 km, the comparable speeds are 0.7 and 24.1 m s^{-1}. Because of the secant squared dependence on zenith angle, at very high cloud bases and large zenith there will be times when the cloud speed is similar to the speed of the solar beam.

With clear skies the irradiance signal is dominated by the solar beam. Diffuse irradiance is around 15% of the total irradiance (at least in the southern plains). With variable cloudiness, the signal fluctuates principally in response to the occurrence or nonoccurrence of clouds intersecting the path between the sun and the pyranometer. When clouds are present along the beam path, the diffuse radiation as a fraction of the signal increases and becomes nearly indistinguishable from the total irradiance in overcast skies. That is, as the irradiance signal decreases due to increasing cloud thickness in the beam path, a correspondingly larger fraction of the sky surrounding the beam path contributes to the irradiance signal. This is shown in Fig. 2 for a clear day, in which the diffuse irradiance is about 15% of the global irradiance; a partly cloudy day, where the diffuse to global ratio is variable but greater than 15%; and a mostly overcast day, where the global and diffuse irradiances are essentially equivalent. Note in Fig. 2 that frequent sampling is necessary to capture the rapid variations in irradiance. In our case, the instantaneous sampling rate is once per second; the samples are then averaged over 1-min intervals to yield the data used in this study.

In summary, the time series of irradiance captures the character of the cloudiness weighted toward the portion of the sky where the sun is located and provides the basis for estimating cloud type. Because the fluctuations due to clouds are in proportion to the clear-sky solar irradiance, which varies systematically during the course of a day, the resulting time series of irradiance

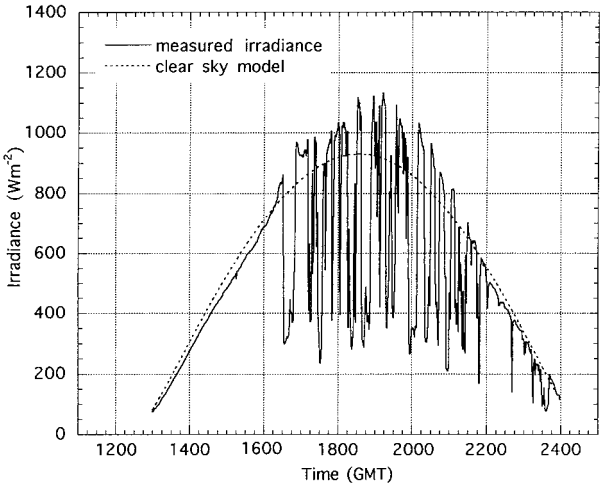

FIG. 3. Measured global irradiance and modeled clear-sky irradiance at Lamont, OK, for 31 March 1995. The data are 1-min averages.

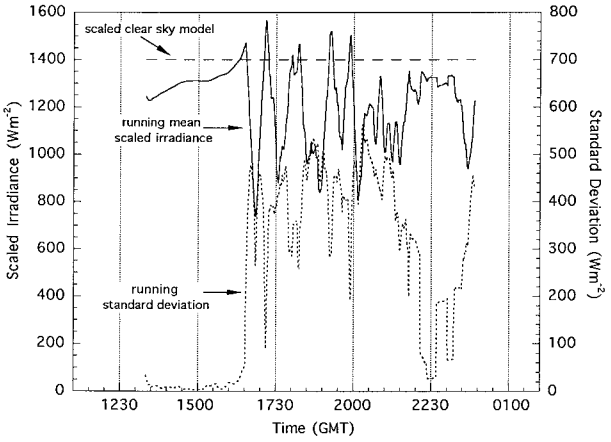

FIG. 4. The solid line is the 21-min running mean and the short dashed line is the 21-min running standard deviation of the observed irradiances in Fig. 3 after they are scaled. The long dashed line is the scaled modeled clear-sky irradiance.

is nonstationary (see Fig. 2b). To make sense of the statistical analysis employed in the classification scheme, it is necessary to linearize the estimated clear-sky and observed irradiances to remove the proportionality. Accordingly, the clear-sky irradiance at each minute of each day is scaled to a constant value, where the scaling function is similarly applied to the observed irradiance. The model for clear-sky irradiance is discussed in section 4.

3. A two-parameter irradiance-based cloud-type classification scheme

a. Obtaining the parameters

The basis for our classification scheme is the premise that certain types of clouds have statistical properties that can be used to identify their occurrence. The seven cloud types and sky conditions that were selected are cumulus, cirrus, cirrus and cumulus, stratus, fog and/or precipitation, no clouds (clear sky), and ''other'' clouds. For simplicity, reference to cloud type in the sequel will include sky conditions.

The first step in the scheme is to scale the modeled clear-sky irradiance discussed later to a constant value of 1400 W m^{-2} for each minute of each day. This value is somewhat greater than the solar constant and never would be exceeded on a cloudless day at any latitude. Because the clear-sky model depends on daily dewpoint and seasonal inputs, each day has a slightly different set of scale factors. The second step is to multiply the observed irradiances by the same set of scale factors. For example, if the measured irradiance were equal to 50% of the clear-sky irradiance, the scaled measured irradiance would be 700 W m^{-2}. The third step is to compute the mean and standard deviation of the scaled measured irradiance in a 21-min moving window.

Figure 3 shows the unscaled, unwindowed clear-sky model and measured irradiance for 31 March 1995. The pyranometer used throughout this study is a periodically calibrated Eppley Precision Spectral Pyranometer with a 1-s time constant (Eppley Laboratory, Inc. 1976). This type of pyranometer has been in use for over 20 years and comprises a thermopile, the upper set of junctions of which responds to the shortwave radiation, and a pair of protective concentric hemispheres of Schott optical glass. The voltage output from the thermopile is proportional to the hemispheric irradiance. The pyranometer of interest is located at the ARM Southern Great Plains (SGP) Calibration and Radiation Testbed (CART) near the town of Lamont (Stokes and Schwartz 1994) in north-central Oklahoma. The solid line denotes consecutive 1-min averages of 60 1-s instantaneous samples of irradiance. The character of the observed irradiance in Fig. 3 reveals that beginning at about 1630 UTC there is sufficient convection to initiate cumulus clouds, which last through much of the remainder of the day. Observed irradiance greater than clear-sky irradiance is a consequence of reflection from the sides of clouds.

Application of scaling and smoothing to Fig. 3 results in the time series of the 21-min running means of 1-min-scaled measured irradiances and the corresponding standard deviations shown in Fig. 4 by the solid and short dashed lines, respectively. The rapid rise in standard deviation coincides with the development of cumulus clouds; simultaneously, the mean scaled irradiance decreases. The horizontal long dashed line is the scaled modeled clear-sky irradiance. The ratio of the running mean scaled irradiance to the scaled clear-sky irradiance and the running standard deviation of scaled observed irradiance in Fig. 4 are the two parameters used in the cloud-type decision criteria.

It should be noted that the window width of 21 min was chosen empirically. A smaller window width, for example, 5 min, acts like a point-in-time measurement,

particularly if a single cloud element persists between the pyranometer and the direct beam for the entire span of the window width. A much larger window, say 50 min, is also inappropriate because different cloud types may occur during this period of time. Based on experiments with various window lengths, 21 min appears to be a reasonable time span for estimating the mean and variance.

b. Decision criteria

Figure 5 shows the decision criteria for each of the seven cloud types. The determination of cloud-type boundaries is based primarily on a comparison of human-observed cloud types coincident with the measured irradiance parameters at the ARM CART site and secondarily on nominal values of the two parameters intuitively expected for the different categories based on the standard cloud-type descriptions. Thus the rectangular boundaries should not be considered as precise delineations.

The lower-left-hand side of Fig. 5 contains stratus, precipitation, and fog. Here the attenuation of solar radiation is high, and the variability in the irradiance signal is small. The large area of cumulus is bounded on the left by a ratio of scaled observed to scaled clear-sky irradiances of 0.5 and on the bottom by a standard deviation of scaled irradiance of about 120 W m^{-2}, which is 20 W m^{-2} higher than the upper-stratus boundary. In addition, there must be at least one value of the 21-min time series that has an irradiance greater than the clear-sky value, as is typical of cumulus clouds (see, for example, Fig. 3). This criterion was used to separate cumulus from cumulus and cirrus, the other large rectangle in Fig. 5. The argument is that cirrus added to cumulus lowers the general level of irradiance relative to clear-sky irradiance to such a value that the above criterion is not met. Nevertheless, the cumulus contribution continues to yield large variance.

Cirrus occupies an area with the ratio of irradiances varying from 0.8 to 1.05. A ratio greater than unity is again due to scattering of the solar beam, this time by patchy cirrus clouds. The standard deviation is low because of the thinness of the clouds and limited attenuation. The clear-sky area is defined by an irradiance ratio extending from 0.88 to 1.05 and a standard deviation of scaled irradiance less than 10 W m^{-2}. The area outside specific cloud types represents clouds of indeterminate types.

The seven cloud types are shown on the left-hand side of Table 1. On the right-hand side are the associated human observations considered acceptable as verification. In section 5 these relationships will be used to compare the objective cloud classification with the human observations for 1995.

4. Clear-sky irradiance model

a. Formulation

Estimating clear-sky solar radiation is one of the primary ingredients of the pyranometer method. The model used here is that developed by Meyers and Dale (1983). The fundamental assumption in this model is that the formulas for transmission of solar radiation through the atmosphere as developed, for example, by Iqbal (1983), for a single wavelength, can be applied to the entire solar spectrum. In the absence of clouds, the surface irradiance I is given by

$$I = I_0 \cos\theta_z T_R T_g T_w T_a, \tag{1}$$

where I_0 is the irradiance at the top of the atmosphere normal to the solar beam; θ_z is the solar zenith angle; and the T_i's are transmission coefficients for Rayleigh scattering (R): permanent gas absorption (g), water vapor absorption (w), and scattering by aerosols (a). Although (1) is generally valid for monochromatic radiation only, it has been widely used to represent broadband irradiance in the real atmosphere (Atwater and Ball 1981). Here, I_0 varies according to time of year as given by Iqbal (1983). The solar zenith angle θ_z is taken from the standard expression given by List (1968, 497) and takes into account latitude, declination angle, and hour angle. The two angles are computed as a function of latitude, longitude, and day of year using an algorithm given by Michalsky (1988).

The Rayleigh and permanent gas scattering and absorption transmission coefficients are taken from Kondratyev (1969) and Atwater and Brown (1974) and given by

$$T_R T_g = 1.021 - 0.084[m(949p \times 10^{-5} + 0.051)]^{0.5}, \tag{2}$$

where p is surface pressure (kPa) and m the optical airmass number at 101.3 kPa given by

$$m = 35(1224 \cos^2\theta_z + 1)^{-0.5}. \tag{3}$$

The water vapor transmission coefficient is

$$T_w = 1 - 0.077(um)^{0.3}, \tag{4}$$

where u is precipitable water (cm) (McDonald 1960). Precipitable water is estimated from the surface dewpoint (Smith 1966) using

$$u = \exp[0.1133 - \ln(\lambda + 1) + 0.0393T_d], \tag{5}$$

where T_d is the local average daily dewpoint (°F) and λ is an empirically derived constant based on season and latitude (Table 2.1 in Smith 1966). The aerosol transmission coefficient was determined by Meyers and Dale (1983) as a residual in clear-sky studies and is given by

$$T_a = x^m, \tag{6}$$

where $x = 0.935$ was found to be nearly constant for continental midlatitude stations.

b. Comparison with observations

Figure 6 shows the percentage difference between modeled [Eq. (1)] and measured clear-sky irradiance given by

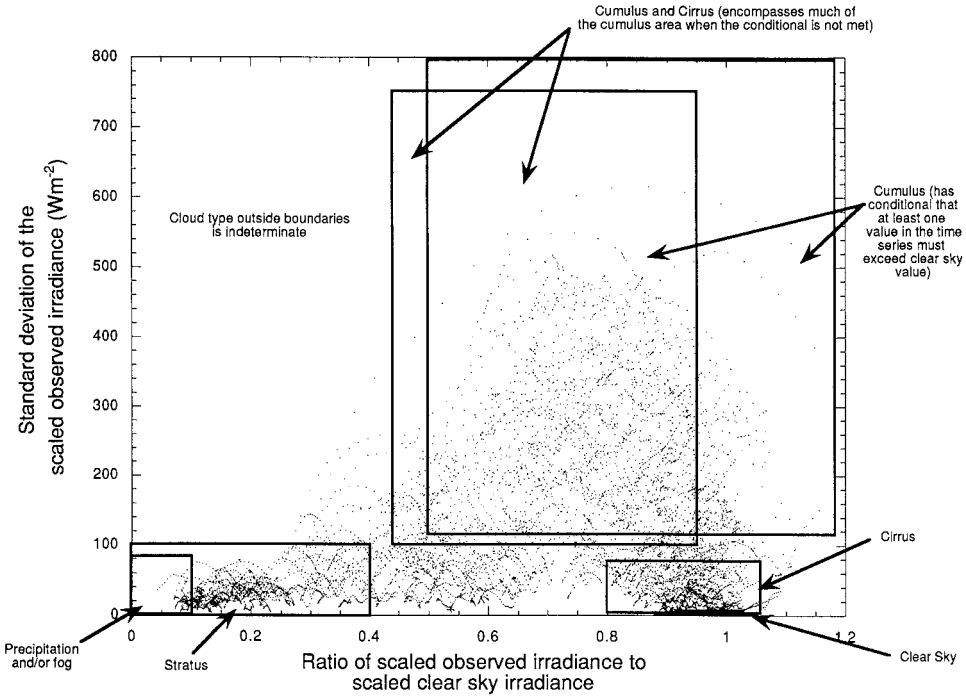

FIG. 5. Decision criteria for estimating cloud type based on the standard deviation of scaled observed irradiance and the ratio of scaled observed irradiance to scaled clear-sky irradiance. The data are 1-min cloud-type estimates for March 1995.

$$\text{percent difference} = \frac{(\text{modeled} - \text{measured})\,\text{clear-sky irradiance}}{\text{measured clear-sky irradiance}} \times 100\% \quad (7)$$

for 12 clear-sky days at the central facility representing all seasons of the year. Five of the days contained haze and utilized a new empirically derived constant for high aerosol content as determined from visibility measurements and human observations (O'Malley 1996). We see that for zenith angles less than 70°, the clear-sky model performs quite well (relative to measurements), capturing the measured clear-sky irradiance within approximately ±5%, except for a few traces. Beyond 70° the differences increase, particularly on the negative side. The differences at large zenith angles may be attributable to a degraded pyranometer cosine response, model error, or both.

Figure 7 shows the numerical differences between the

TABLE 1. The human observations (right-hand side) considered acceptable as verification of the seven cloud types (left-hand side) derived from the pyranometer method.

Cloud type defined by pyranometer method	Matching cloud type from human observations
Clear sky	No cloud reported
Cirrus	Any high clouds of 0.1 to 1.0 coverage
Cumulus	Any low and/or midlevel cumuloform clouds with 0.1 to 0.8 coverage
Cirrus and cumulus	Any high clouds of 0.1 to 1.0 coverage and any low or midlevel cumuloform clouds of 0.1 to 1.0 coverage
Stratus	Any low or midlevel clouds of 0.9 to 1.0 coverage
Precipitation and/or fog	Precipitation reported and/or sky obscured by fog
Indeterminate or other	Multiple levels containing different cloud types

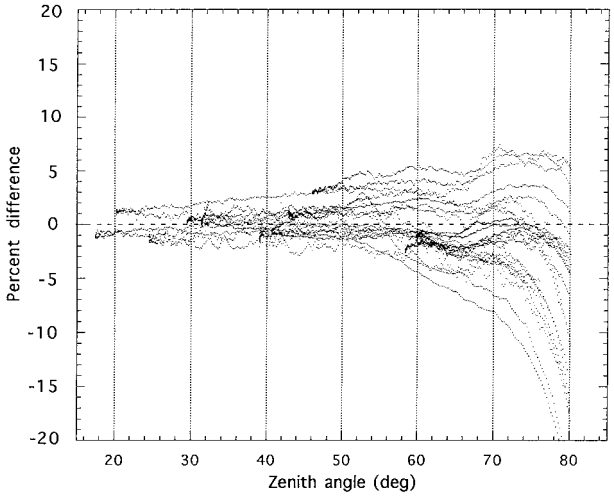

FIG. 6. Percent difference of (modeled − measured)/measured irradiances for 12 clear days in all seasons of 1995.

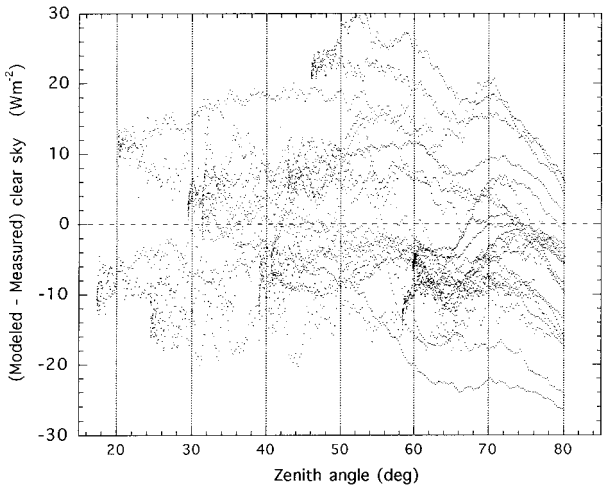

FIG. 7. Numerical differences between modeled and measured clear-sky irradiance for the days in Fig. 6.

modeled and measured clear-sky irradiance for the same days as in Fig. 6. It is apparent that there is an uncertainty of about ± 30 W m^{-2} in the clear-sky model relative to the pyranometer observations that is independent of zenith angle. Model minus measured differences are most likely due to using a constant aerosol transmission coefficient, surface dewpoint as a proxy of total column water vapor, and an inexact seasonal parameter λ [see Eq. (5)].

5. Comparison of pyranometer cloud-type estimation with human observations

a. Background

It must be recognized at the outset that in comparing cloud types from a pyranometer with those from human observations, the methods of measurement are fundamentally different. In the latter, the entire sky or at least a sizable portion is viewed at a moment in time; in the former, the estimation is weighted toward the solid angle traversed by clouds passing through the solar beam over a period of time (21 min). Nevertheless, if one or more cloud types are approximately uniformly distributed across the sky, there should be good correspondence between the two methods. We can anticipate that there will be times when, for example, widely scattered cumulus do not interrupt the solar beam, resulting in the pyranometer method underestimating the occurrence of cumulus. In fact, since human cloud observations are based on a large fraction or the totality of the sky, the pyranometer method, in general, will underestimate cloudiness determined by the human method.

One means to assess the efficacy of the pyranometer method of cloud classification is by comparing cloud types produced from the pyranometer with those from human observations. Human observations are taken by the central facility operator, who records cloud types and height using the World Meteorological Organization cloud-type-code for each quadrant of the sky (NE, SE, SW, and NW) at the beginning of each hour on weekdays during most daylight hours. Given that the sun is always located in the southern half of the sky at the central facility, the comparisons were made in the SE quadrant before solar noon and in the SW quadrant following solar noon. Table 1 provides the connection between the objective determination of cloud type and human observations. For example, if the observer notes any type of high cloud between 0.1 and total coverage, and the objective method yields cirrus, a ''correct'' decision is declared. Similarly, a correct decision is made if the observer records any low or midlevel clouds covering 0.9 or 1.0 coverage and the objective method indicates stratus. The terms ''correct'' and ''incorrect'' are used in the sense of having a match or not of the left side to the right side of Table 1. That is, human observations are used as the reference, but since they are subjective, different observers can classify similar clouds differently.

b. Comparisons among no clouds, cirrus, cumulus, and cirrus and cumulus

Contingency Tables 2–4 provide a representative selection of monthly cloud-type classification comparisons for 1995. If there was always a one-to-one correspondence, then the values of all the off-diagonal el-

TABLE 2. Contingency table showing comparison of cloud type estimated by pyranometer method vs cloud type from human observations for January 1995.

	Cloud type from pyranometer method						
	No clouds	Cirrus	Cumulus	Cirrus and cumulus	Stratus	Precipitation–fog	Other
Cloud type from human observation							
No clouds	22	3	0	0	0	0	0
Cirrus and	2	5	0	0	0	0	0
Cumulus	6	11	8	8	6	0	11
Cirrus and cumulus	7	4	11	7	0	0	2
Stratus	0	0	0	3	21	0	12
Precipitation–fog	0	0	0	0	3	4	6
Other	0	0	1	0	0	0	4

TABLE 3. Same as Table 2 but for August 1995.

	Cloud type from pyranometer method						
	No clouds	Cirrus	Cumulus	Cirrus and cumulus	Stratus	Precipitation–fog	Other
Cloud type from human observation							
No clouds	50	49	0	0	0	0	2
Cirrus	0	1	0	0	0	0	0
Cumulus	4	20	29	12	1	0	5
Cirrus and cumulus	2	2	2	4	0	0	0
Stratus	0	0	0	1	10	1	5
Precipitation–fog	0	0	0	1	6	6	0
Other	0	0	6	2	0	0	3

ements of each contingency table would be zero. Overall, the pyranometer method and human observations agree about 45% of the time. An examination of the off-diagonal elements shows that the two human-observed cumulus and cirrus and cumulus categories generally get distributed among the four pyranometer determined no clouds, cirrus, cumulus, and cirrus and cumulus categories. There are two principal causes for the differences. One is that in the pyranometer method, the analysis is weighted toward the sun's position, as described in section 2. As a result, there will be 21-min periods in which the pyranometer method indicates no clouds (or a clear sky, as defined in Fig. 5) crossing the solar beam, while the human observer sees cumulus or cirrus or cirrus and cumulus away from the solar beam. Similarly, when cirrus or cumulus are determined from the pyranometer method, cumulus or cirrus, respectively, also can be visually observed away from the solar beam, yielding cirrus and cumulus from human observations.

The second main source of differences is atmospheric aerosol content. The end effect is that cirrus and cirrus and cumulus will be predicted by the pyranometer method when, in fact, only aerosols or aerosols and cumulus are present. These conditions can be observed especially in August 1995 (Table 3). Our conclusions with regard to aerosol effects are based on an investigation of cirrus overestimation on eight hazy, cloud-free days during July and August 1995. We found that the differences between modeled and observed clear-sky irradiances ranged from 0 to 75 W m^{-2} throughout the day, about twice the range in Fig. 7 and from other model studies (Coakley et al. 1983). From our investigation a new value, $x = 0.895$, in (6) was found to best estimate the observed irradiance on these hazy, clear days. The new constant is used in the classification when hazy days are present. However, we also found that aerosols and thin cirrus have similar standard deviations of scaled observed irradiance. An example is shown in Fig. 8 in which the observer reported clear skies with noticeable haze and reduced visibility. In Fig. 9 the observer reported cirrus but no haze or reduced visibility. The irradiance signal in both figures is quite similar. Because of similar standard deviations, the cloud-type estimation still falls in the cirrus category, as seen in Fig. 5, even though the corrected ratio of scaled observed irradiance to scaled clear-sky irradiance is employed. As a consequence of aerosols and the weighting by the solar beam described in the previous paragraph, the pyra-

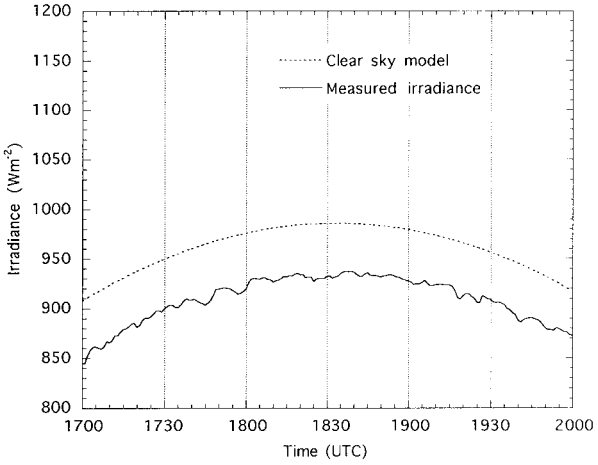

FIG. 8. Clear-sky model and observed irradiances in the presence of aerosols in an otherwise cloudless sky.

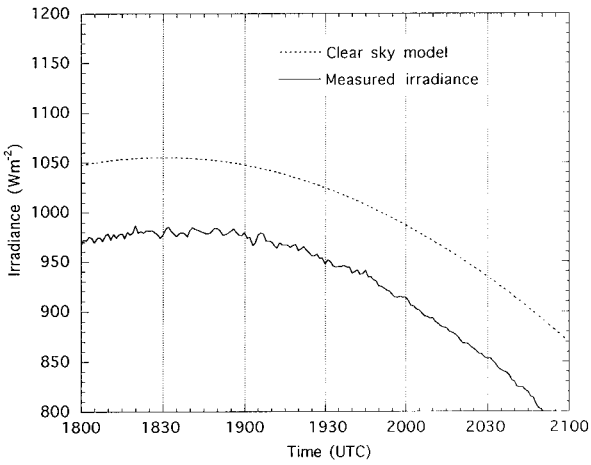

FIG. 9. Clear-sky model and observed irradiances on a day when thin cirrus was present.

TABLE 4. Same as Table 2 but for November 1995.

	Cloud type from pyranometer method						
	No clouds	Cirrus	Cumulus	Cirrus and cumulus	Stratus	Precipitation–fog	Other
Cloud type from human observation							
No clouds	26	10	0	0	0	0	0
Cirrus	2	5	3	0	0	0	0
Cumulus	10	8	13	8	1	0	3
Cirrus and cumulus	4	9	7	3	0	0	2
Stratus	1	0	0	4	5	0	3
Precipitation–fog	0	0	0	1	0	0	2
Other	3	2	14	3	0	0	3

nometer method can predict cirrus when the human observer records only cumulus (as shown in Tables 2–4).

c. Comparisons among pyranometer ''other'' and cumulus and stratus

Table 2, especially, shows that there are a number of occurrences in which the pyranometer method produces ''other'' cloud type, while the cloud type derived from human observation is cumulus or stratus. With regard to the other–cumulus comparison, it was initially thought that the differences were due to viewing the sides of cumulus at large zenith angles. An investigation showed that while this can be case, the differences occurred at all times of day. It was thought also that the other–stratus differences were due to sharp cloud boundaries but, again, this was not always the case. The explanation is as follows.

At the outset of the comparison effort, a number of decisions were made concerning how to provide a useful comparison of the two methods. One in particular dealt with classifying stratocumulus clouds. During winter months at the SGP site, stratocumulus clouds are frequently reported. Because the pyranometer method cannot be used to classify stratocumulus due to the wide range in irradiance signal from effectively cumuloform to stratiform clouds, for comparison purposes, we classified the observer-reported stratocumulus into two categories. If the reported stratocumulus coverage was 8/10 or less, we classified the observation as cumulus; if the stratocumulus coverage was 9/10 or 10/10, it was classified as stratus. The former criterion corresponds to traditional broken and scattered clouds, the latter to overcast conditions.

In Fig. 5 stratocumulus clouds occur in a band extending from approximately the center of the stratus area upward to the right to include the lower left 1/9 of the cumulus area. Most of the occurrences of other–cumulus and other–stratus mismatches arose when stratocumulus was reported, and the pyranometer method yielded values of irradiance ratios between 0.40 and 0.65 and standard deviations between 25 and 80 W m^{-2}, that is, the space to the right of the stratus area and below the cumulus area in Fig. 5.

In the majority of cases of reported stratocumulus for 1995, however, a favorable comparison occurred. That is, most of the cumulus and stratus classified from stratocumulus clouds by the scheme described above lie within the cumulus and stratus areas, respectively, as determined by the pyranometer method.

d. Other differences

Other systematic differences occur. Table 2 for January 1995 shows six occurrences of stratus from the pyranometer method and cumulus from the human observer. Some other months (not shown) indicate similar values. Many of these differences occur when stratocumulus was reported. Thus the pyranometer method predicted cumulus (stratus), while the stratocumulus classification scheme yielded stratus (cumulus). Table 3 for August 1995 shows six occurrences of stratus from the pyranometer method and precipitation–fog by the observer. This discrepancy results because the same irradiance conditions can occur for both heavy stratus and precipitation–fog, while Fig. 5 shows a unique separation between them.

In Table 4, November 1995, there are 14 cases in which the pyranometer method yields cumulus when the human observer classification is other. These differences arise from having three cloud layers (low, middle, high). Due to the transition from when the sun path is essentially clear to when it is completely blocked, the standard deviation exceeds 100 W m^{-2}. Due to scattering from the sides of cumulus clouds, the measured irradiance exceeds clear-sky irradiance and the irradiance ratio for the 21-min window is greater than 0.5. As seen in Fig. 5, the pyranometer method will classify the cloud type as cumulus.

6. Combining categories

Figure 10 shows the frequency of occurrence of the seven cloud types using the pyranometer method and the human observer method for each month in Tables 2–4. The frequency of occurrence is defined as the ratio of the column (or row) sums, as appropriate, to the sum of column (or row) sums. Among these, as well as the

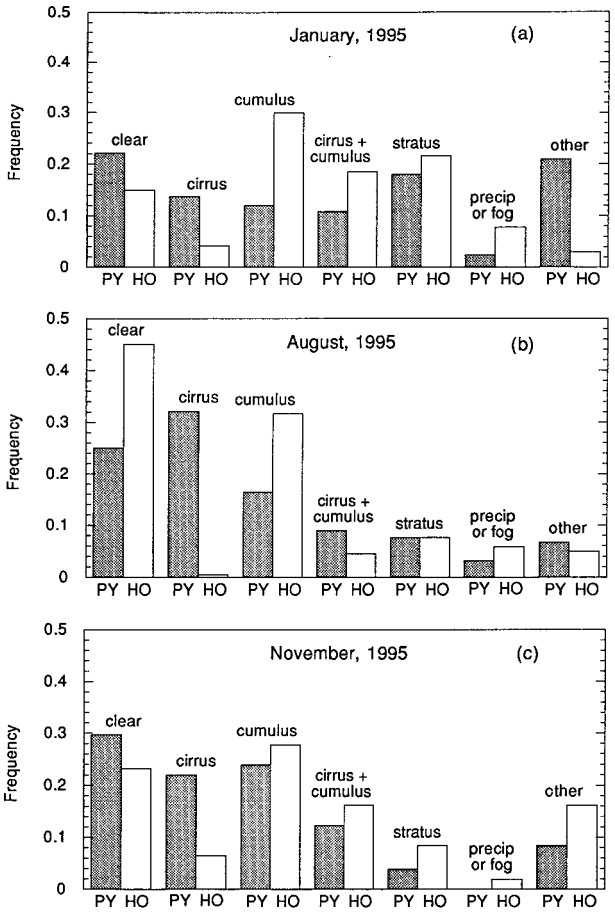

FIG. 10. Frequency of occurrence of the seven cloud types using the pyranometer (PY) method and the human observer (HO) method from Tables 2–4 for (a) January, (b) August, and (c) November.

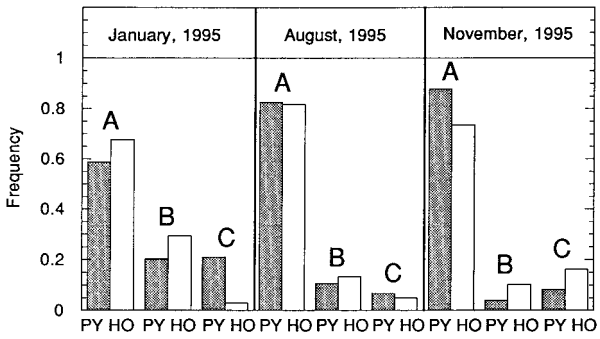

FIG. 11. Combining the seven categories into three categories for each of the three months in Fig. 10. Category A includes clear skies, cumulus, cirrus, and cirrus and cumulus; category B is stratus and precipitation and/or fog; and category C is other.

remaining months of 1995, the frequency of occurrence of clear (no clouds) and cirrus clouds is typically higher from the pyranometer method than from human observation. The former is inherent in the pyranometer method, the latter is a consequence of aerosols. Exceptions occur with high aerosol content, for example, in August and October (not shown), in which the occurrence of clear skies from the pyranometer method is substantially reduced. Invariably (including months not shown), the frequency of occurrence of cumulus from the pyranometer method is less than that from human observations, again, because the irradiance in the pyranometer method is weighted toward solar beam path. There seems to be no systematic difference between the frequency of occurrence for cirrus and cumulus from the two methods when all months are examined. The same can be said of stratus. The frequency of occurrence for precipitation–fog from the pyranometer method is usually less than that from human observations.

Figure 11 shows the results of combining the seven categories into three categories for each of the three months. For each month note that the sky conditions that include clear, cirrus, cumulus, and cirrus and cumulus occur 60% to about 90% of the time, while the remaining time is roughly equally shared between the categories for stratus and precipitation and/or fog. This distribution is similarly observed for other months of the year. In this coarse classification the differences in frequency of occurrence between the irradiance-based and human-observed clouds vary from essentially 0 to 0.15 in the other category in January. The irradiance-based and observed clouds are very similar in category A, in contrast to the differences seen among the individual cloud types in Fig. 10, in large part because aerosol effects occur only in category A and are therefore averaged out. The range of differences shown for these three months applies to other months of the year as well.

7. Summary and conclusions

The purpose of the research described in this paper was to determine whether a simple and inexpensive scheme could be developed to determine continuous daytime cloud type. If such was the case a means would be available to provide cloud-type data at remote locations or locations in general where no human observations are available. The method, called the pyranometer method, involves a statistical analysis of time series of 1-min-averaged pyranometer observations and knowledge of the clear-sky irradiance. The statistics computed are the standard deviation of irradiance over a 21-min window and the ratio of average irradiance relative to clear-sky irradiance. The two statistics are entered into a nomogram to yield cloud type. The entire process can be automated.

In comparing cloud types from the pyranometer method with those from simultaneous human observations we found agreement about 45% of the time. The reasons for this figure are as follows. Very different methods of cloud-type estimation are employed: one is weighted toward clouds traversing the sun, and the other is a wide-angle summation. The consequence is that the pyranometer method will underestimate the occurrence of

cloudiness relative to a human observer. We noted also that aerosols can fool the pyranometer method into classifying an otherwise clear sky into cirrus because the time series of their irradiances can be quite similar, as shown in Figs. 8 and 9. As best as we can determine, many of the mismatches in our comparison study occur because of aerosols. The estimation of aerosols using only a pyranometer is not possible. More elaborate instrumentation is required. In the case of haze in the planetary boundary layer (PBL), ASOS visibility measurements may be useful to document its occurrence so that a corrective measure can be taken. In the case of aerosols within or above the PBL, Harrison and Michalsky (1994) describe a ground-based method to estimate optical depth. Unfortunately, the added cost of the associated instrumentation is prohibitive to widespread installation.

Stratocumulus presents a special problem because its appearance varies from nearly cumuloform to nearly stratiform. For comparison purposes a simple algorithm was designed to classify stratocumulus as either cumulus or stratus, depending on fractional cloud cover estimated by the observer. While this approach usually is successful, cloud-type mismatches between the two methods do occur. Last, because sharp boundaries separate cloud-type categories, as seen in Fig. 5, small differences in the two statistical properties can lead to a mismatch between the observer classification and that by the pyranometer method.

Apart from the aerosol problem, we are not aware of any intrinsic reason the cloud-type classification developed here and shown in Fig. 5 cannot be applied at other locations. In general, we expect the pyranometer method to provide a more accurate report of cloud type at lower rather than higher latitudes. This is because the solar beam is passing through more of the vertical depth of the cloud(s) than slant thickness. It is evident that in locations where aerosols are a common feature, such as in the southern plains, identification of a simple and effective means to account for them would significantly improve the cloud-type classification using the pyranometer method.

In conclusion, an analysis of the time series of irradiance from a pyranometer can provide a useful assessment of cloud type where none is otherwise available but is desired. The method has merit with respect to the applications identified in section 1, but will always be limited to estimating cloud type in only a portion of the sky. Solving the aerosol problem will require additional instrumentation.

Acknowledgments. This research was supported by the Environmental Sciences Division of the U.S. Department of Energy (through Battelle PNNL Contract 144880-A-Q1 to the Cooperative Institute for Mesoscale Meteorological Studies) as part of the Atmospheric Radiation Measurement Program.

REFERENCES

Atwater, M. A., and P. S. Brown, 1974: Numerical computations of the latitudinal variation of solar radiation for an atmosphere of varying opacity. *J. Appl. Meteor.,* **13,** 289–297.

——, and J. T. Ball, 1981: A surface solar radiation model for cloudy atmospheres. *Mon. Wea. Rev.,* **109,** 878–888.

Barnett, T. P., J. Ritchie, J. Foat, and G. Stokes, 1998: On the space–time scales of the surface solar radiation field. *J. Climate,* **11,** 88–96.

Bland, W. L., 1996: Uncertainty of daily insolation estimates from a mesoscale pyranometer network. *J. Atmos. Oceanic Technol.,* **13,** 255–261.

Brock, F. V., K. C. Crawford, R. L. Elliott, G. W. Cuperus, S. J. Stadler, H. L. Johnson, and M. D. Eilts, 1995: The Oklahoma Mesonet: A technical review. *J. Atmos. Oceanic Technol.,* **12,** 5–19.

Coakley, J. A., R. D. Cess, and F. B. Yurevich, 1983: The effect of tropospheric aerosols on the earth's radiation budget: A parameterization for climate models. *J. Atmos. Sci.,* **40,** 116–138.

Eppley Laboratory, Inc., 1976: Instrumentation for the measurement of the components of solar and terrestrial radiation. Eppley Laboratory, Inc., Newport, RI, 12 pp.

Harrison, L., and J. Michalsky, 1994: Objective algorithms for the retrieval of optical depths from ground-based measurements. *Appl. Opt.,* **33,** 5126–5132.

Iqbal, M., 1983: *An Introduction to Solar Radiation.* Academic Press, 390 pp.

Kondratyev, K. Ya., 1969: *Radiation in the Atmosphere.* Academic Press, 912 pp.

List, R. J., 1968: *Smithsonian Meteorological Tables.* 6th ed. Smithsonian Institution Press, 527 pp.

McDonald, J. E., 1960: Direct absorption of solar radiation by atmospheric water vapor. *J. Meteor.,* **17,** 319–328.

Meyers, T. P., and R. F. Dale, 1983: Predicting daily insolation with hourly cloud height and coverage. *J. Climate Appl. Meteor.,* **22,** 537–545.

Michalsky, J. J., 1988: The Astronomical Almanac's algorithm for approximate solar position (1950–2050). *Sol. Energy,* **40,** 227–235.

O'Malley, M. S., 1996: Determining daytime radiation and cloud climatologies from time series of surface irradiances from the ARM/CART Central Facility. M.S. thesis, School of Meteorology, University of Oklahoma, 109 pp. [Available from School of Meteorology, University of Oklahoma, Norman, OK 73019.]

Rossow, W. B., and R. A. Schiffer, 1991: ISCCP cloud data products. *Bull. Amer. Meteor. Soc.,* **72,** 2–20.

Smith, W. L., 1966: Note on the relationship between total precipitable water and surface dewpoint. *J. Appl. Meteor.,* **5,** 726–727.

Stokes, G. M., and S. E. Schwartz, 1994: The Atmospheric Radiation Measurement (ARM) program: Programmatic background and design of the cloud and Radiation test bed. *Bull. Amer. Meteor. Soc.,* **75,** 1201–1221.